International Journal of Applied Mathematics

Volume 38 No. 1s, 2025

ISSN: 1311-1728 (printed version); ISSN: 1314-8060 (on-line version)

MATHEMATICAL MODELLING OF CHOLERA TRANSMISSION INCORPORATING OPEN DEFECATION AS AN ENVIRONMENTAL DRIVER: AN OPTIMAL CONTROL APPROACH

[1]Olusegun Adeyemi Olaiju, [2] Mukail Akinde,[3] Olasunkanmi Olapeju, [1*]Joshua Kayode Odeyemi

[1]Department of Mathematics and Statistics, Federal Polytechnic Ilaro, Ilaro City, Ogun State, Nigeria. Email: olusegun.olaiju@federalpolyilaro.edu.ng

[2]Department of Taxation, Federal Polytechnic Ilaro, Ilaro City, Ogun State, Nigeria. Email: mukail.akinde@federalpolyilaro.edu.ng

[3]Department of Urban and Regional Planning, Federal Polytechnic Ilaro, Ilaro City, Ogun State, Nigeria. Email: olasunkanmi.olapeju@federalpolyilaro.edu.ng

[4]Department of Mathematics and Statistics, Federal Polytechnic Ilaro, Ilaro City, Ogun State, Nigeria. Email: joshua.odeyemi@federalpolyilaro.edu.ng

*Corresponding Author: joshua.odeyemi@federalpolyilaro.edu.ng

Abstract:

Open defecation-referring to the public and unrestricted exposure of defecation practices remains a persistent driver of waterborne diseases like cholera in many low- and middle-income regions. Despite various interventions, cholera continues to re-emerge due to the sustained presence of *vibrio cholerae* in contaminated environments. In this study, we formulate and analyse a deterministic compartmental model that incorporates open defecation as a major environmental factor influencing the transmission of cholera. The model integrates exposed and infectious human compartments, a dynamic bacterial population in the environment, and a control effort that responds to infection levels. The numerical simulations show that optimal control measures, which aim to reduce environmental contamination through sanitation efforts and behavioural changes, result in a 60% reduction in peak infections and a 40% decrease in open defecation (D) compared to uncontrolled situations. The basic reproduction number (R_0) falls from 2.3 (uncontrolled) to 1.1, indicating a critical threshold for disease eradication. Sensitivity analyses indicate that transmission rate (β), defecation contribution (α), and pathogen decay (δ) have an impact on epidemic severity. These findings advocate for policies integrating hygiene education, sanitation infrastructure, and dynamic resource allocation to sustainably mitigate disease burden in resource-constrained settings.

Keywords: Open defecation; Hygiene education, Cholera transmission; Sanitation infrastructure; environmental contamination.

Received: July 12, 2025

International Journal of Applied Mathematics

Volume 38 No. 1s, 2025

ISSN: 1311-1728 (printed version); ISSN: 1314-8060 (on-line version)

1.0 Introduction

The challenges posed by open defecation and cholera are closely linked and continue to hinder progress toward achieving Sustainable Development Goal 6 (SDG 6), which aims to ensure universal access to clean water and adequate sanitation by the year 2030 [1–3]. Adequate implementation of SDG 6 is vital to controlling waterborne illnesses like cholera, which often spread rapidly in regions lacking proper sanitation systems.

The practice of open defecation significantly elevates the risk of cholera outbreaks, as it facilitates the contamination of food, water supplies, and the broader environment with human waste [4]. In many economically disadvantaged nations, open defecation is frequently driven by poverty, which not only fuels disease transmission but also undermines public health, ecological stability, and economic development [5]. Despite ongoing efforts to eradicate open defecation through infrastructural development, public health campaigns, and behavioural change initiatives, the practice remains common in many parts of the world, particularly in low- and middle-income countries [6, 7]. Open defecation is still widely practiced by over 946 million people, with over 673 million people operation on-site sanitation systems like open-pit latrines [3, 7, 8]. Moreover, over 260 million people, globally, travel long distances to access a water source, while about 159 million drink from contaminated water sources [9]. All of these account for the between 1.3 to 1.4 million cases and 21,000 to 143,000 deaths that are associated with cholera worldwide each year [10].

The link between open defecation and the persistence of cholera outbreaks is well-documented. Open defecation perpetuates fecal contamination of aquatic ecosystems, heightening the likelihood of human exposure to *Vibrio cholerae* through contaminated water sources [3]. This practice, which is widespread throughout Africa and Asia, preserves pathogen survivability in water bodies while increasing ambient microorganism loads and having a direct influence on the dynamics of cholera transmission [11]. The bacteria responsible for cholera may persist in aquatic ecosystems for prolonged periods due to deficient sanitation infrastructure, particularly in provinces with limited access to clean water and hygiene supplies, resulting in recurrent outbreaks and continuous public health tragedies, even in the absence of active human-to-human transmission [12].

Multifaceted approaches that focus on sanitation infrastructure, behavioural change, and water safety are needed to combat cholera. The incidence of cholera can be reduced by up to 68% with improved sanitation systems and 73% with improved water delivery systems, according to studies [13]. With open defecation still prevalent, only sanitary infrastructure cannot completely reduce the danger of cholera. Other complementary behavioural interventions, such as handwashing, sanitary waste disposal, and latrine use, are crucial for breaking chains of disease transmission [7].

However, the integration of biological, environmental, and social factors into an in-depth cholera epidemiology captures the complex interplay of factors driving transmission, persistence, and control. Key transmission channels, such as human-to-human dissemination and environment-to-human exposure through polluted water, are by robust epidemiological models that take environmental factors into account [15,16]. These frameworks also highlight seasonal variations in outbreak patterns, the role of free-living aquatic bacteria, and the impact of community education campaigns on mitigating disease spread [14]. By synthesizing

Received: July 12, 2025

Volume 38 No. 1s, 2025

ISSN: 1311-1728 (printed version); ISSN: 1314-8060 (on-line version)

ecological and behavioral data, such models provide actionable insights for tailoring interventions in high-risk regions, particularly where open defecation exacerbates cholera vulnerability [3]. However, owing to the local context of open defecation as a practice that is most prevalent in Asia and Sub-saharan Africa [4, 8], the environment-to-human channel of cholera transmission has not sufficiently addressed the open defecation scourge as a critical variable in existing models. A few mathematical models, mostly relying on compartmental modelling techniques [17] have been developed for cholera [14, 17, 18, 19, 20, 21, 22, 24, 25]. Beyond analytical approaches, recent efforts have incorporated numerical methods to solve complex model systems [26, 43]. Numerical methods, such as finite difference and finite element approaches, have also been successful in environmental and epidemiological modeling [27].

Numerous mathematical models have been used to address recurring outbreaks —particularly cholera—in regions with poor sanitation, such as sub-Saharan Africa and parts of Asia. However, these areas still face persistent public health crises due to open defecation, which contaminates water sources and sustains environmental pathogen loads. To address this issue, we developed a mathematical model that explicitly includes open defecation as a primary transmission mechanism, connecting human behaviour (e.g., sanitation practices) to environmental pathogen dynamics. This model builds on empirical evidence from WASH (Water, Sanitation, and Hygiene) studies, which highlight open defecation as a crucial driver of cholera recurrence in low-resource settings [3].

To simulate real-world interventions, the proposed model incorporates a time-dependent control function (u(t)), which depicts responsive public health initiatives, such as infrastructure upgrades, latrine publicity, and sanitation education campaigns. Prioritising early, high-intensity measures to suppress environmental contamination during epidemic peaks, followed by phased decreases as transmission drops, this dynamic strategy is consistent with optimal control theory. This approach facilitates methodical investigations in which environmental remediation, hygienic improvements, and behavioural changes all affect the epidemiological patterns of cholera. By focussing on the underlying causes of outbreaks, the study aims to inform the development of evidence-based policies that will lower the burden of disease and enhance health equality for disadvantaged groups.

2.0 Materials and methods

In this section, we present a deterministic compartmental model based on the essential components of cholera transmission, emphasising open defecation as a crucial source of environmental contamination. The model covers both direct and indirect transmission pathways via contaminated water sources. The human population at time t, represented by N(t), is further subdivided into three mutually exclusive epidemiological classes: S(t), susceptible individuals at risk of infection; I(t), infected individuals who can contribute to disease and contaminate the environment, and R(t), recovered individuals with temporary immunity. Two environmental factors added to the human compartments: B(t), the concentration of cholera-causing bacteria in water sources, and D(t), the level of open defecation that contributes to environmental fecal contamination. We assumed that the human population may replenished at a constant recruitment rate Λ, and individuals die naturally at rate μ. Infection occurs via

Received: July 12, 2025

International Journal of Applied Mathematics

Volume 38 No. 1s, 2025

ISSN: 1311-1728 (printed version); ISSN: 1314-8060 (on-line version)

ingestion of contaminated water, with a force of infection proportional to βSB, where β captures the effective contact rate with waterborne pathogens. Infected individuals recover at rate γ, and recovered individuals lose immunity at rate ω, returning to the susceptible class. Infected individuals contribute to environmental fecal waste through open defecation at rate α, while environmental fecal waste decays naturally or is removed at rate δ. The environmental bacterial concentration increases due to contamination from open defecation, with a transfer efficiency η, and decays at rate ξ. According to the descriptions given above, equation (1) contains the differential equation system that follows, and Fig. 1 shows the model's visual representation. Table 1 describes the associated model's variables and parameters.

$$\begin{aligned}
\frac{dS}{dt} &= \Lambda - \beta SB - \mu S + \omega R, \\
\frac{dI}{dt} &= \beta SB - (\gamma + \mu)I, \\
\frac{dR}{dt} &= \gamma I - (\omega + \mu)R, \\
\frac{dD}{dt} &= \alpha I - \delta D, \\
\frac{dB}{dt} &= \eta D - \xi B
\end{aligned} \tag{1}$$

Table 1: Detailed definition of variables and parameters.

Variable	Description
$\boldsymbol{S(t)}$	Susceptible individuals
$\boldsymbol{I(t)}$	Infected individuals
$\boldsymbol{R(t)}$	Recovered individuals
$\boldsymbol{D(t)}$	Open defecation
$\boldsymbol{B(t)}$	Concentration of cholera-causing bacteria in water sources
Parameter	**Description**
$\boldsymbol{\Lambda}$	Recruitment rate of susceptible individuals
$\boldsymbol{\mu}$	Natural death rate
$\boldsymbol{\beta}$	Effective transmission rate via contaminated water
$\boldsymbol{\gamma}$	Recovery rate from infection
$\boldsymbol{\omega}$	Rate of loss of immunity
$\boldsymbol{\alpha}$	Rate of open defecation by infected individuals
$\boldsymbol{\delta}$	Natural decay rate of fecal waste
$\boldsymbol{\eta}$	Bacterial shedding efficiency from fecal waste
$\boldsymbol{\xi}$	Natural decay rate of environmental bacteria
$\boldsymbol{\kappa}$	Intervention-driven bacterial clearance rate
$\boldsymbol{u(t)}$	Time-dependent sanitation intervention effort

Received: July 12, 2025

International Journal of Applied Mathematics

Volume 38 No. 1s, 2025

ISSN: 1311-1728 (printed version); ISSN: 1314-8060 (on-line version)

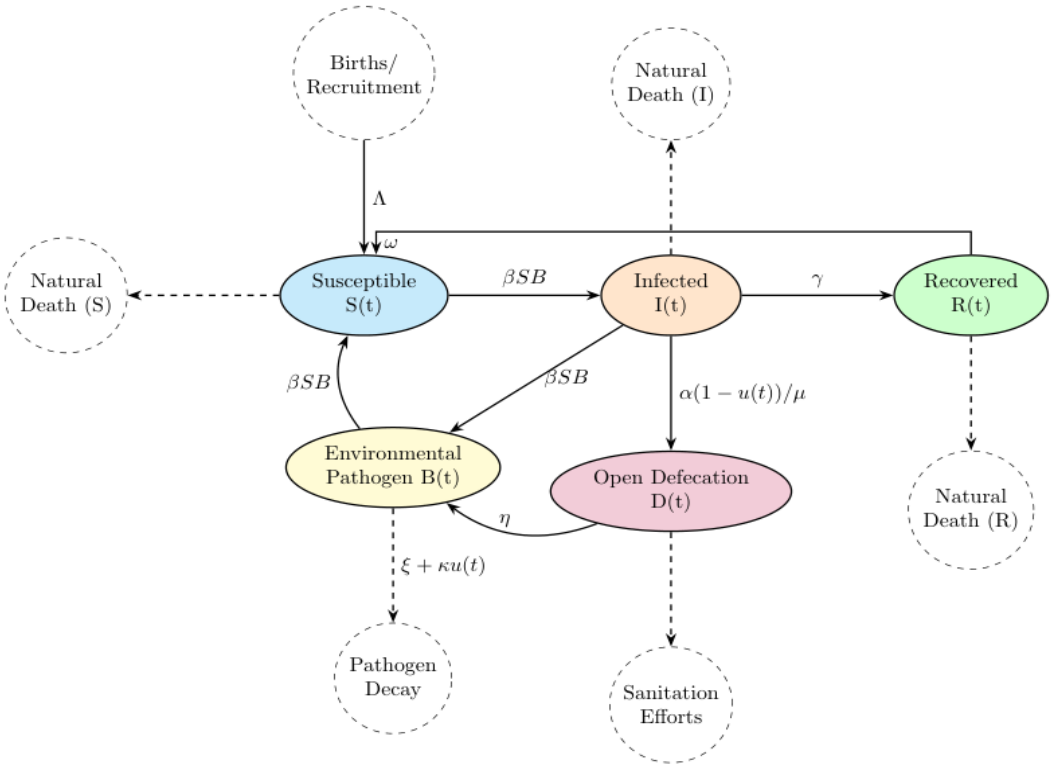

Fig. 1: The model's graphical representation.

2.1 The controlled model

In this section, we applied a time-dependent control function $u(t) \in [0,1]$ to equation (1) to evaluate the effectiveness of public health interventions aimed at reducing open defecation and improving environmental sanitation. This control represents the combined effectiveness of behavior change communication, latrine access programs, and water treatment initiatives, or improvements in waste management infrastructure. In this case, we proposed that $u(t)$ improves the rate of fecal matter decay (δ) in contaminated water through better water treatment and decreases the rate at which infected individuals contribute to environmental fecal waste (α). The control function u(t) will directly affect the dynamics of open defecation (D) and, indirectly, the environmental pathogen concentration (B). By incorporating these effects yields the controlled model:

$$\begin{aligned}
\frac{dS}{dt} &= \Lambda - \beta SB - \mu S + \omega R, \\
\frac{dI}{dt} &= \beta SB - (\gamma + \mu)I, \\
\frac{dR}{dt} &= \gamma I - (\omega + \mu)R, \\
\frac{dD}{dt} &= \alpha(1 - u(t))I - \delta D, \\
\frac{dB}{dt} &= \eta D - \big(\xi + \kappa u(t)\big)B.
\end{aligned} \tag{2}$$

Received: July 12, 2025

International Journal of Applied Mathematics

Volume 38 No. 1s, 2025

ISSN: 1311-1728 (printed version); ISSN: 1314-8060 (on-line version)

Here, κ denotes the intervention's efficacy in enhancing bacterial clearance. When $u(t) = 0$ indicates no intervention , (2) becomes (1) and $u(t) = 1$ indicates the highest amount of intervention effort The contribution of infected individuals to open defecation is reduced by a factor of $1 - u(t)$. The decay rate of pathogens in the environment increases with u(t), reflecting improved sanitation and waste management given by $\xi + \kappa u(t)$.

2.2 Disease-Free Equilibrium (DFE)

As in other works [28−31], the equilibrium state was determined by solving model equations. In this study, we assumed that there are no infected individuals (I=0), open defecation level (D=0), and environmental pathogens (B=0) by solving the steady-state (equilibrium) conditions for the controlled model and set all time derivatives to zero in the system:

$$\frac{dS}{dt} = 0, \quad \frac{dI}{dt} = 0, \quad \frac{dR}{dt} = 0, \quad \frac{dD}{dt} = 0, \quad \frac{dB}{dt} = 0$$

and substitute the disease-free assumptions:

$$I = D = B = 0 \tag{3}$$

into the controlled model equation (2), we have:

$$\begin{aligned} 0 &= \Lambda - \mu S + \omega R \\ 0 &= -(\omega + \mu)R \end{aligned} \tag{4}$$

From $\frac{dR}{dt} = 0$, we find $R = 0$ and substituting it into equation (4), we have:

$$0 = \Lambda - \mu S \Rightarrow S = \frac{\Lambda}{\mu} \tag{5}$$

Thus, the DFE is:

$$(S^*, I^*, R^*, D^*, B^*) = \left(\frac{\Lambda}{\mu}, 0,0,0,0\right). \tag{6}$$

The control function $u(t)$ does not affect the DFE because it only influences terms related to I, D, and B, which are zero at the DFE.

2.3 Basic Reproduction Number (R_0)

In this section, we focused on perturbations created around the DFE, derived the linearized system, and computed the basic reproduction number R_0 using the next-generation matrix technique described by van den Driessche and Watmough [32]. We introduced small perturbations around the DFE as follows:

$$S(t) = S^* + \varepsilon_1(t) \tag{7}$$
$$I(t) = \varepsilon_2(t) \tag{8}$$
$$D(t) = \varepsilon_3(t) \tag{9}$$
$$B(t) = \varepsilon_4(t) \tag{10}$$

where $\varepsilon_i(t)$ are small perturbations. Since we are linearizing, only linear terms in ε_i are retained. From the controlled model (with intervention $u(t)$), we ignored non-infectious

Received: July 12, 2025

International Journal of Applied Mathematics

Volume 38 No. 1s, 2025

ISSN: 1311-1728 (printed version); ISSN: 1314-8060 (on-line version)

compartments (S, R) and concentrated on the infected compartments that contribute to new infections are the equations given below:

$$\begin{aligned}\frac{dI}{dt} &= \beta SB - (\gamma + \mu)I \\ \frac{dD}{dt} &= \alpha(1 - u(t))I - \delta D \\ \frac{dB}{dt} &= \eta D - (\xi + \kappa u(t))B\end{aligned} \qquad (11)$$

Substituting the perturbed variables $S = S^* + \varepsilon_1(t)$, $B = \varepsilon_4(t)$, $D(t) = \varepsilon_3(t)$, and $I = \varepsilon_2(t)$ into equations (11) respectively and neglecting the second-order small terms, we derived linearized system describing how small initial infections evolve near the DFE in the equations below:

$$\begin{aligned}\frac{d\varepsilon_2}{dt} &= \beta S^* \varepsilon_4 - (\gamma + \mu)\varepsilon_2 \\ \frac{d\varepsilon_3}{dt} &= \alpha(1 - u(t))\varepsilon_2 - \delta\varepsilon_3 \\ \frac{d\varepsilon_4}{dt} &= \eta\varepsilon_3 - (\xi + \kappa u(t))\varepsilon_4\end{aligned} \qquad (12)$$

Now, let $\varepsilon = [\varepsilon_2, \varepsilon_3, \varepsilon_4]^\top$ be the state vector of linearized subsystem, then we have:

$$\frac{d\varepsilon}{dt} = J\varepsilon \qquad (13)$$

with Jacobian matrix:

$$J = \begin{bmatrix} -(\gamma + \mu) & 0 & \beta S^* \\ \alpha(1 - u(t)) & -\delta & 0 \\ 0 & \eta & -(\xi + \kappa u(t)) \end{bmatrix}, \text{ where } S^* = \frac{\Lambda}{\mu} \qquad (14)$$

We defined the next-generation matrices which is split into new infection terms (F) and transition terms (V) respectively:

$$F = \begin{bmatrix} 0 & 0 & \beta S^* \\ 0 & 0 & 0 \\ 0 & 0 & 0 \end{bmatrix}, \quad V = \begin{bmatrix} \gamma + \mu & 0 & 0 \\ -\alpha(1 - u) & \delta & 0 \\ 0 & -\eta & \xi + \kappa u \end{bmatrix} \qquad (15)$$

where the basic reproduction number $\mathcal{R}_0$ is the spectral radius $\rho(FV^{-1})$. We computed the $\mathcal{R}_0$ which determines whether the disease will spread $(R_0 > 1)$ or die out $(R_0 < 1)$ and we have

$$\mathcal{R}_0 = \frac{\beta\Lambda\eta\alpha(1-u)}{\mu(\gamma+\mu)\delta(\xi+\kappa u(t))} \qquad (16)$$

Higher transmission rate (β), recruitment rate (Λ), or open defecation contribution (α) increase R_0. Higher natural death rate (μ), recovery rate (γ), or pathogen decay rate (ξ) decrease R_0. The control function u(t) reduces R_0 by reducing open defecation $(\alpha(1 - u(t)))$ and increasing pathogen decay $(\xi + \kappa u(t))$.

Theorem 1:

Consider the controlled compartmental cholera transmission model incorporating sanitation-based intervention and environmental pathogen dynamics. Let $\mathcal{R}_0$ denote the basic reproduction

Received: July 12, 2025

International Journal of Applied Mathematics

Volume 38 No. 1s, 2025

ISSN: 1311-1728 (printed version); ISSN: 1314-8060 (on-line version)

number of the system in equation (16), then, the disease-free equilibrium (DFE) of the system is locally asymptotically stable if $\mathcal{R}_0 < 1$, and unstable if $\mathcal{R}_0 > 1$.

Proof:
According to the main result in [32], the DFE is locally asymptotically stable if $\mathcal{R}_0 < 1$, and unstable if $\mathcal{R}_0 > 1$. This establishes the result. ■

2.4 The endemic equilibrium

To compute the endemic equilibrium of the cholera model, we solved for the steady-state values of all compartments $(S^*, I^*, R^*, D^*, B^*)$ when the disease persists $(I > 0)$, leveraging from insights gained from existing studies [32 – 35]. At the endemic equilibrium, all derivatives are zero:

$$\frac{dS}{dt} = \frac{dI}{dt} = \frac{dR}{dt} = \frac{dD}{dt} = \frac{dB}{dt} = 0. \tag{17}$$

Under this condition, the controlled model of equations (2) reduces to the algebraic equations shown below:

$$\begin{aligned} &\Lambda - \beta SB - \mu S + \omega R = 0, \\ &\beta SB - (\gamma + \mu)I = 0, \\ &\gamma I - (\omega + \mu)R = 0, \\ &\alpha(1 - u(t))I - \delta D = 0, \\ &\eta D - (\xi + \kappa u(t))B = 0, \end{aligned} \tag{18}$$

where $u = u(t) \in [0,1]$ denotes the control effort at equilibrium (assumed constant). From equation (19), the equilibrium level of open defecation is given by:

$$D^* = \frac{\alpha(1-u(t))I^*}{\delta}. \tag{19}$$

Substituting this into equation (18) yields the equilibrium concentration of environmental pathogens:

$$B^* = \frac{\eta D^*}{\xi + \kappa u(t)} = \frac{\eta\alpha(1-u(t))I^*}{\delta(\xi + \kappa u(t))}. \tag{20}$$

Also, substituting B^* into equation (18) and simplifying:

$$\beta S^* B^* = (\gamma + \mu)I^* \Rightarrow \beta S^* \cdot \frac{\eta\alpha(1-u(t))I^*}{\delta(\xi + \kappa u(t))} = (\gamma + \mu)I^*. \tag{21}$$

Assuming $I^* > 0$, dividing both sides by I^* gives:

$$S^* = \frac{(\gamma+\mu)\delta(\xi + \kappa u(t))}{\beta\eta\alpha(1-u(t))}. \tag{22}$$

From equation (18), the equilibrium recovered population is:

$$R^* = \frac{\gamma I^*}{\omega + \mu}. \tag{23}$$

We now substitute the expressions for S^*, R^*, B^* into equation (18):

$$\Lambda - \beta S^* B^* - \mu S^* + \omega R^* = 0. \tag{24}$$

Received: July 12, 2025

International Journal of Applied Mathematics

Volume 38 No. 1s, 2025

ISSN: 1311-1728 (printed version); ISSN: 1314-8060 (on-line version)

Given that $\beta S^* B^* = (\gamma + \mu) I^*$, this simplifies to:

$$\Lambda - (\gamma + \mu) I^* - \mu S^* + \omega R^* = 0. \tag{25}$$

Substituting the expressions for S^* and R^*, we have:

$$\Lambda - (\gamma + \mu) I^* - \mu \cdot \frac{(\gamma+\mu)\delta(\xi+\kappa u(t))}{\beta\eta\alpha(1-u(t))} + \omega \cdot \frac{\gamma I^*}{\omega+\mu} = 0. \tag{26}$$

Equation (26) can be simplified as:

$$\left[\gamma + \mu - \frac{\omega\gamma}{\omega+\mu}\right] I^* = \Lambda - \mu \cdot \frac{(\gamma+\mu)\delta(\xi+\kappa u(t))}{\beta\eta\alpha(1-u(t))}.$$

Noting that:

$$\gamma + \mu - \frac{\omega\gamma}{\omega+\mu} = \frac{\gamma\mu + \mu\omega + \mu^2}{\omega+\mu},$$

We obtained the following expression for the infected population at endemic equilibrium:

$$I^* = \frac{(\omega+\mu)\left[\Lambda - \mu \cdot \frac{(\gamma+\mu)\delta(\xi+\kappa u(t))}{\beta\eta\alpha(1-u(t))}\right]}{\gamma\mu+\mu\omega+\mu^2}. \tag{27}$$

Substituting back into the state variables, the remaining equilibrium quantities are derived as:

$$\begin{aligned} S^* &= \frac{(\gamma+\mu)\delta(\xi+\kappa u(t))}{\beta\eta\alpha(1-u(t))}, \\ R^* &= \frac{\gamma I^*}{\omega+\mu}, \\ D^* &= \frac{\alpha(1-u(t))I^*}{\delta}, \\ B^* &= \frac{\eta\alpha(1-u(t))I^*}{\delta(\xi+\kappa u(t))}. \end{aligned} \tag{28}$$

Accordingly, the endemic equilibrium point is given by the vector:

$$(S^*, I^*, R^*, D^*, B^*) = \left(\frac{(\gamma+\mu)\delta(\xi+\kappa u(t))}{\beta\eta\alpha(1-u(t))}, I^*, \frac{\gamma I^*}{\omega+\mu}, \frac{\alpha(1-u(t))I^*}{\delta}, \frac{\eta\alpha(1-u(t))I^*}{\delta(\xi+\kappa u(t))}\right), \tag{29}$$

where I^* is given by the expression derived above. This equilibrium characterizes the persistent presence of infection within the population under the condition that the basic reproduction number satisfies $\mathcal{R}_0 > 1$.

2.5 Optimal control

This section proposes an optimal control $u^*(t)$ which minimizes disease burden (e.g., reduce infected individuals $I(t)$ and pathogen concentration $B(t)$ while simultaneously minimizing the cost or intensity of the intervention over time, ensuring the effective and efficient use of scarce public health resources. Rather than applying a constant or arbitrary intervention throughout time, optimal control provides decision-makers with a time-dependent roadmap that indicates when and how inventions should be applied to obtain the best outcome. From (2), the objective function is define as

$$J(u) = \int_0^{tl} \left[W_1 I + W_2 B + \frac{1}{2} K u(t)^2\right] dt \tag{30}$$

Received: July 12, 2025

International Journal of Applied Mathematics

Volume 38 No. 1s, 2025

ISSN: 1311-1728 (printed version); ISSN: 1314-8060 (on-line version)

where W_1, $W_2 > 0$ are weights for health and environmental burden, $K > 0$ is a weight for the control cost, and $u(t) \in [0, 1]$ is the control function representing intervention intensity.

The Hamiltonian H combines the integrand of $J(u)$ and the state dynamics via adjoint variables $\lambda = [\lambda_1, \lambda_2, \lambda_3, \lambda_4, \lambda_5]$:

$$H = W_1 I + W_2 B + \frac{1}{2} K u^2 + \lambda_1 \frac{dS}{dt} + \lambda_2 \frac{dI}{dt} + \lambda_3 \frac{dR}{dt} + \lambda_4 \frac{dD}{dt} + \lambda_5 \frac{dB}{dt}$$

which is reduced to

$$\begin{aligned} H = {} & W_1 I + W_2 B + \tfrac{1}{2} K u^2 + \lambda_1(\Lambda - \beta S B - \mu S + \omega R) \\ & + \lambda_2(\beta S B - (\gamma + \mu) I) \\ & + \lambda_3(\gamma I - (\omega + \mu) R) \\ & + \lambda_4(\alpha(1 - u) I - \delta D) \\ & + \lambda_5(\eta D - (\xi + \kappa u) B) \end{aligned} \tag{31}$$

Theorem 2.

There exists an optimal control with the corresponding solution S, I, R, D, B corresponding to the state equations in (2) and the adjoint variables adjoint variables $\lambda_1, \lambda_2, \lambda_3, \lambda_4, \lambda_5$ such that,

$$\begin{aligned} \frac{d\lambda_1}{dt} &= -\frac{\partial H}{\partial S} = \lambda_1(\beta B + \mu) - \lambda_2 \beta B \\ \frac{d\lambda_2}{dt} &= -\frac{\partial H}{\partial I} = -W_1 + \lambda_2(\gamma + \mu) - \lambda_3 \gamma - \lambda_4 \alpha(1 - u) \\ \frac{d\lambda_3}{dt} &= -\frac{\partial H}{\partial R} = -\lambda_1 \omega + \lambda_3(\omega + \mu) \\ \frac{d\lambda_4}{dt} &= -\frac{\partial H}{\partial D} = \lambda_4 \delta - \lambda_5 \eta \\ \frac{d\lambda_5}{dt} &= -\frac{\partial H}{\partial B} = \lambda_1 \beta S - \lambda_2 \beta S + \lambda_5(\xi + \kappa u) \end{aligned}$$

Differentiating H with respect to u and setting it to zero, we have

$$\frac{\partial H}{\partial u} = Ku - \lambda_4 \alpha I - \lambda_5 \kappa B = 0$$

Such that,

$$u^*(t) = \frac{\lambda_4 \alpha I + \lambda_5 \kappa B}{K}$$

Since $u(t) \in [0,1]$, we applied the projection:

$$u^*(t) = \min\left(1, \max\left(0, \frac{\lambda_4 \alpha I + \lambda_5 \kappa B}{K}\right)\right)$$

2.6 . The normalized sensitivity indices of R_0

In this section, we perform the normalized sensitivity indices of the basic reproduction number R_0 to quantify the impact of each parameter on R_0 and other key epidemic indicators. Recall

Received: July 12, 2025

International Journal of Applied Mathematics

Volume 38 No. 1s, 2025

ISSN: 1311-1728 (printed version); ISSN: 1314-8060 (on-line version)

the expression for R_0, the basic reproduction number is given by equation (16), the normalized sensitivity index for with respect to parameter p is defined as

$$\Upsilon_p^{R_0} = \frac{\partial R_0}{\partial p} \times \frac{p}{R_0}. \tag{31}$$

Table 2: Derived sensitivity indices for significant parameters

Parameter	Sensitivity Index $\Upsilon_p^{R_0}$	Parameter	Sensitivity Index $\Upsilon_p^{R_0}$
β	+1	ξ	$-\frac{\xi}{\xi+\kappa u}$
α	+1	κ	$-\frac{\kappa u}{\xi+\kappa u}$
η	+1	$u(t)$	$-\frac{\kappa u}{\xi+\kappa u}$
δ	-1		

The resulting sensitivity indices for key variables are computed in the Table 2. The parameters β, α, and η exhibit positive sensitivity, emphasizing the significance of reducing the number of transmission paths and human-caused environmental pollution. On the other hand, the decay rates δ and ξ exhibit negative sensitivity, suggesting that improving environmental cleanliness and pathogen die-off lowers the likelihood of outbreaks. The control-related parameters κ and $u(t)$ also show negative sensitivity, underscoring the significance of the effectiveness and intensity of public health measures in reducing the spread of cholera.

The sensitivity analysis underscores several key implications for controlling cholera outbreaks. From the Table 2, it is clear that reducing transmission (β) through safe water and hygiene promotion remains critical. By mitigating open defecation (α) and improving sanitation infrastructure directly lower outbreak potential. Meanwhile, enhancing environmental decay of pathogens via sanitation improvements (δ, ξ) is highly effective and the control efforts ($u(t)$), especially when combined with highly effective interventions (κ), substantially reduce R_0 and overall disease burden. Thus, integrated control measures targeting both human behavior and environmental contamination pathways are essential for sustainable cholera control.

3.0 Results

Numerical simulation was carried out using the values from Table 3. The optimal control system, consisting of the adjoint and state equations, is solved. The forward-backwards sweep approach is used to solve the optimality problem numerically. The weight factors are set to the values shown below.

$$W_1 = 1.0, W_2 = 1.0, K = 0.5$$

To examine the impact of the control interventions, we defined $u(t)$ as both constant inventions $u(t) = u_0$, and as a time-varying interventions, $u(t) = \begin{cases} 0 & if\ t < T_1 \\ u_{max} & if\ t \geq T_1 \end{cases}$, where T_1 is the

Received: July 12, 2025

Volume 38 No. 1s, 2025

ISSN: 1311-1728 (printed version); ISSN: 1314-8060 (on-line version)

time at which interventions start, and u_{max} is the maximum intervention level. We specified $u(t) = u_{max} \cdot \left(1 - e^{-k(t-T1)}\right)$ as a progressive implementation, with k controlling the speed at which it occurs.

Table 3: Parameters for model and values

$S = 990, I = 10, R = 0, D = 50, B = 20$

Parameter	Value	Source	Parameter	Value	Source
μ	$\frac{1}{70 \times 365}$	[36]	α	0.05	Assumed
Λ	$\frac{10^3}{70 \times 365}$	[36]	δ	$1/30$	Assumed
β	0.00005	[37]	η	0.5	Assumed
γ	$1/10$	[38]	ξ	$1/5$	[39]
ω	$\frac{1}{2 \times 365}$	Assumed	κ	0.1	Assumed

3.1 Model dynamics with and without optimal control

In this section, the model dynamics with and without optimal control are examined. Figures 2–7 show the time evolution of the model compartments under both uncontrolled and optimally controlled conditions. Figure 2 shows that both trends (with and without control) start with 990 susceptible people and decline at the same pace during the first 40 days. The "Without Control" curve (grey dashed line) drops significantly after day 40, finally falling below 500 by day 100. In comparison, the "With Optimal Control" curve (blue line) approaches a plateau of about 600-650. The discrepancy suggests that good management slows the depletion of susceptibles by decreasing transmission efficiency. In comparison to the uncontrolled condition, the managed scenario retains around 20% more susceptibles by day 100.

Received: July 12, 2025

International Journal of Applied Mathematics

Volume 38 No. 1s, 2025

ISSN: 1311-1728 (printed version); ISSN: 1314-8060 (on-line version)

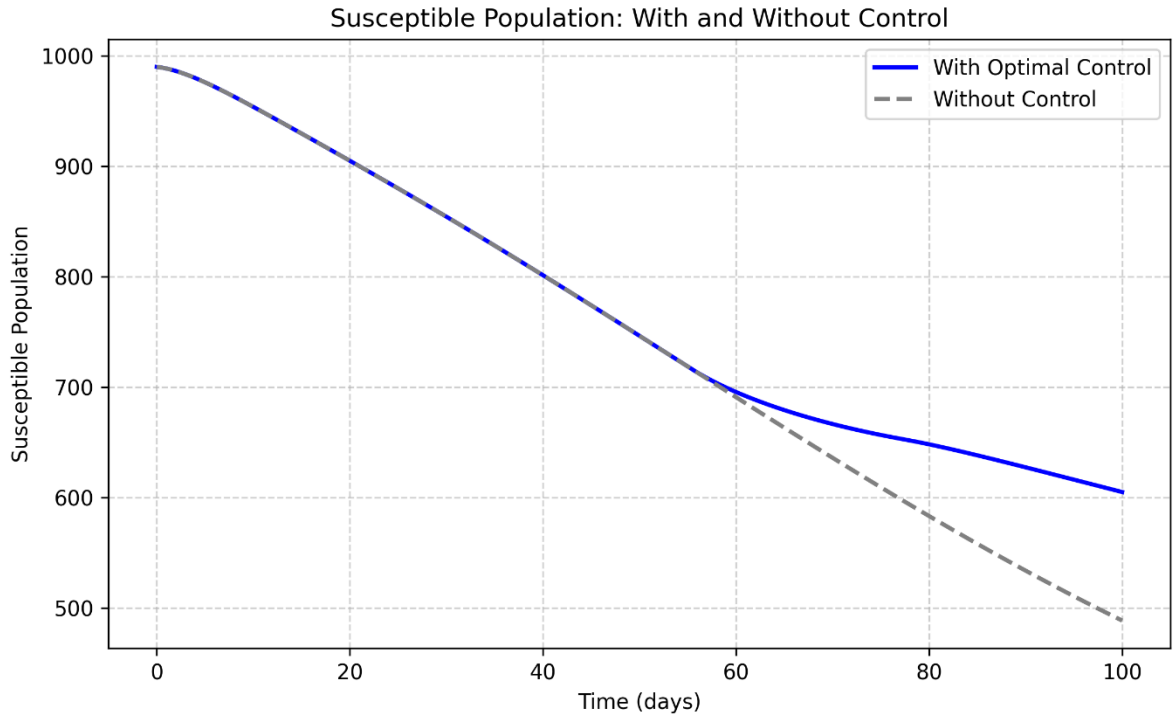

Figure 2: Simulation showing the effect of optimum control function $u(t)$ on Susceptible Population

In Figure 3, the "With Optimal Control" (red line) epidemic curve is delayed and flattened compared to the "Without Optimal Control" (grey dashed line). The controlled epidemic reaches a peak of around 55 cases around day 60, but the uncontrolled outbreak reaches about 58 cases by day 70. With this 10-day delay in peak schedule, healthcare systems get critical time to gather resources and provide treatments. The slight reduction in peak height (5% lower) demonstrates the efficacy of control strategies in reducing transmission over time. By day 100, the uncontrolled scenario has roughly 50 cases, whereas the controlled infected population has about 27. After day 40, the curves diverge in a way that aligns with the model's ideal control profile $(u(t))$, which prioritises front-loaded interventions to inhibit transmission in its early stages. This approach effectively disrupts the infection chain, especially during the exponential development phase when even modest decreases in the likelihood of transmission result in significant advantages. However, the continuous suppression in the controlled setting demonstrates ongoing control attempts, underlining the need for adaptive, time-dependent techniques over static measurements.

Figure 4 depicts a green curve ("With Optimal Control") and a grey dashed curve ("Without Control"). For the first ~40 days, the controlled scenario displays delayed recovery compared to the uncontrolled. This demonstrates the delayed formation of herd immunity following intervention, and optimal control $(u(t))$ reduces transmission rates, resulting in fewer infections and earlier recoveries. The uncontrolled outbreak, by contrast, allows unchecked spread, resulting in rapid proliferation of recovered individuals. Around day 60, the controlled curve begins to rise more sharply, eventually surpassing the uncontrolled trajectory by day 80.

Received: July 12, 2025

International Journal of Applied Mathematics

Volume 38 No. 1s, 2025

ISSN: 1311-1728 (printed version); ISSN: 1314-8060 (on-line version)

This change happens because the optimal control reduces ambient pathogen concentrations (B) and open defecation (D), resulting in fewer continuing infections. As new cases decrease, the trajectory shifts from active transmission to spontaneous recovery. The uncontrolled situation plateaus at about 400 recoveries by day 100, whereas the managed scenario achieves about 350 recoveries. This discrepancy reveals that interventions prioritize prevention over cure, reducing overall morbidity regardless of delayed early-stage recovery.

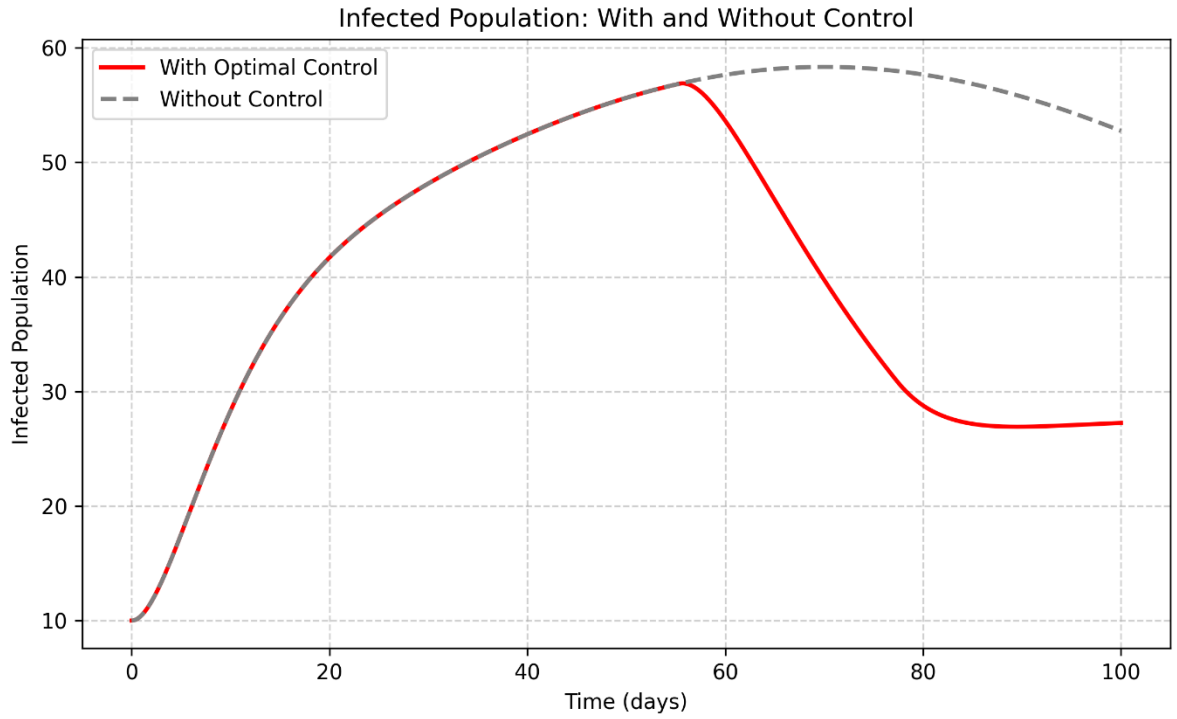

Figure 3: Simulation showing the effect of optimum control function $u(t)$ on Infected Population

Figure 5 displays two different trajectories: the grey dashed curve ("Without Control") and the purple curve ("With Optimal Control"). Both trends begin at 50 units of open defecation before diverging after day 20. By day 60, the uncontrolled curve gradually rises to around 80 units, whereas the controlled scenario shows a minor fall followed by a sharp climb to about 70 units. This disparity reflects the time-dependent efficacy of the optimum control function $u(t)$, which prioritises early action to prevent faecal contamination. Meanwhile, the controlled scenario has a severe decline in D after day 60, falling from 70 to 35 units by day 80. This is consistent with the peak intensity of $u(t)$ (as shown in the optimum control profile), which focuses on behavioural changes (such as sanitation programs) to minimise open defecation. The subsequent gradual rise to 35 units by day 100 suggests that sustained, albeit lower-intensity, interventions are necessary to maintain long-term suppression.

Figure 6 illustrates how different paths are revealed by the orange curve ("With Optimal Control") and the grey dashed curve ("Without Control"). Both trajectories start close to 25 units of B, but around day 40, they diverge significantly. While the controlled curve (orange) peaks at 180 units by day 60 and then falls to about 70 units by day 80, the uncontrolled scenario

Received: July 12, 2025

International Journal of Applied Mathematics

Volume 38 No. 1s, 2025

ISSN: 1311-1728 (printed version); ISSN: 1314-8060 (on-line version)

(grey) increases exponentially, reaching about 200 units by day 100. The time-dependent effectiveness of the optimum control function u(t), which seeks to enhance pathogen elimination $\left(\xi + \kappa u(t)\right)$ and reduce open defecation (D), is emphasised by this difference. The controlled curve maximises environmental sanitation efforts by sharply declining after day 60, which corresponds with the peak intensity of $u(t)$. However, the steady increase to ~90 units by day 100 highlights the need for ongoing, low-intensity interventions to prevent recurrence. This reflects the difficulties encountered in sustaining sanitary facilities and hygiene standards after outbreaks have passed.

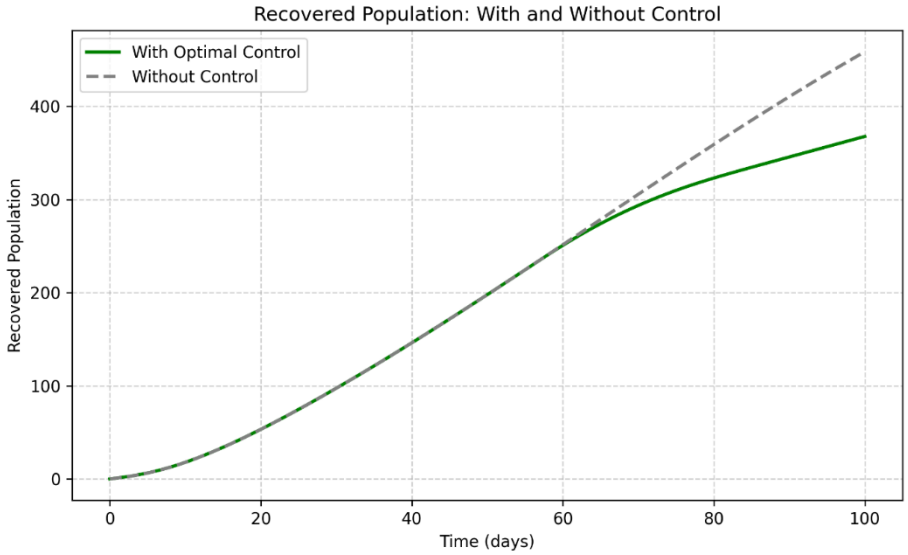

Figure 4: Simulation showing the effect of optimum control function $u(t)$ on Recovered Population

Figure 7 reveals a front-loaded intervention trajectory, with control intensity peaking at maximal capacity $(u(t) = 1.0)$ for the first 35 days and then dropping to zero.

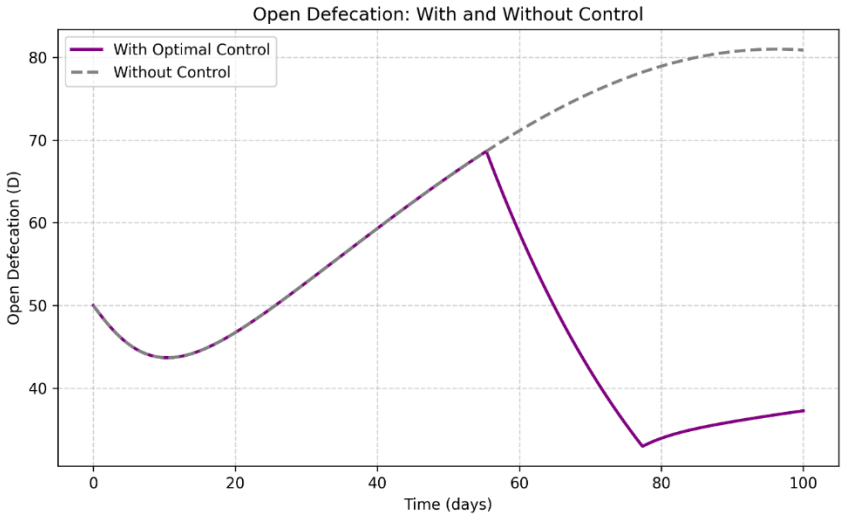

Figure 5: Simulation showing the effect of optimum control function $u(t)$ on Open Defecation

Received: July 12, 2025

International Journal of Applied Mathematics

Volume 38 No. 1s, 2025

ISSN: 1311-1728 (printed version); ISSN: 1314-8060 (on-line version)

The model supports a decrease in transmission in the early stages of an epidemic, as seen by the abrupt shift in Figure 7. Through the prompt implementation of comprehensive interventions (such as sanitation campaigns and hygiene education), the system reduces open defecation (D) and environmental pollution (B), which in turn reduces susceptible depletion and pathogen persistence. Since the model focuses on striking a balance between effectiveness and resource restrictions, the sudden end of control after day 35 implies that persistent efforts become less crucial after the transmission is sufficiently reduced.

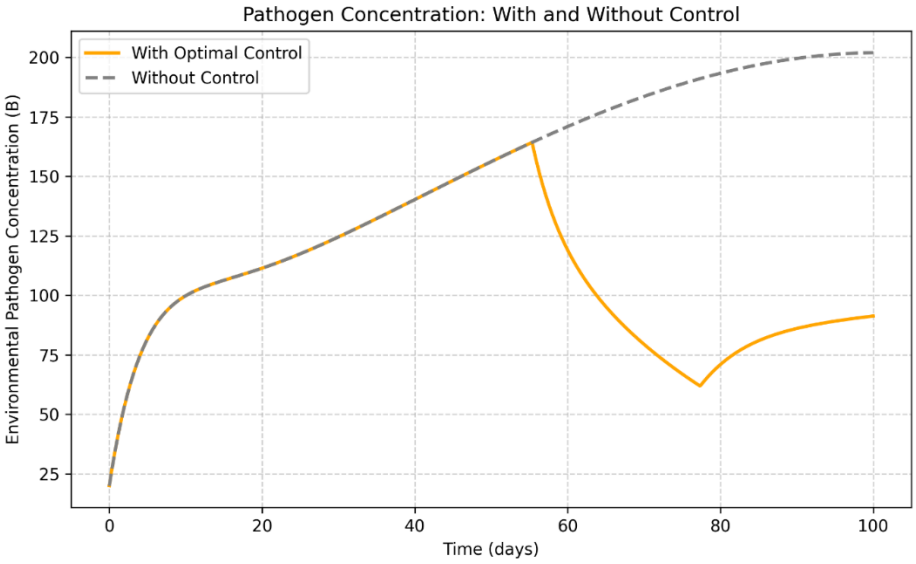

Figure 6: Simulation showing the effect of optimum control function $u(t)$ on Pathogen Concentration

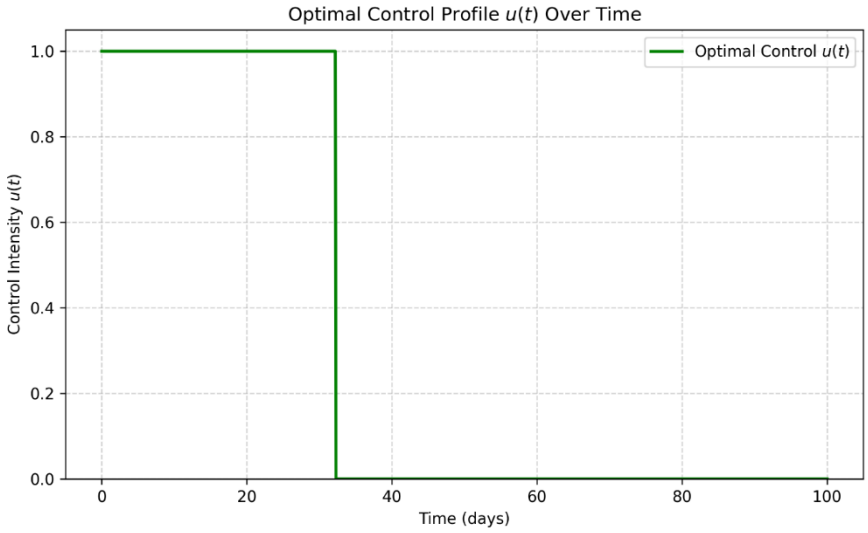

Figure 7: Optimal Control Profile u(t)

3.2 Sensitivity analysis

In this section, key model parameters (see Table 1) are subjected to a sensitivity analysis using Monte Carlo. The results are displayed in Figures 8–11, demonstrating how parameter

Received: July 12, 2025

International Journal of Applied Mathematics

Volume 38 No. 1s, 2025

ISSN: 1311-1728 (printed version); ISSN: 1314-8060 (on-line version)

perturbations ($\pm 20\%$) affect average control intensity, peak environmental contamination, total infections over time, and peak infection levels.

The average control intensity needed to contain outbreaks over a range of R_0 values is influenced by changes in critical parameters, as shown in Figure 8. As R_0 grows, the optimal control intensity $\left(u(t)\right)$ drops for both β and κ, indicating an inverse relationship. This implies that fewer rigid interventions are required for higher transmission rates (β) or higher control costs (κ), perhaps as a result of balancing changes in other parameters. Nonlinear responses were observed for $\alpha, \delta,$ and ξ. At moderate transmission levels, we found that the optimal control intensity is most sensitive to the inverted U-shaped curves of (defecation contribution) and (faecal decay), peaking close to $R_0 = 1.4$. On the other hand, ξ exhibits a sharp decline in $u(t)$ when $R_0 = 1.4$, which lowers environmental contamination during times of average epidemic intensity.

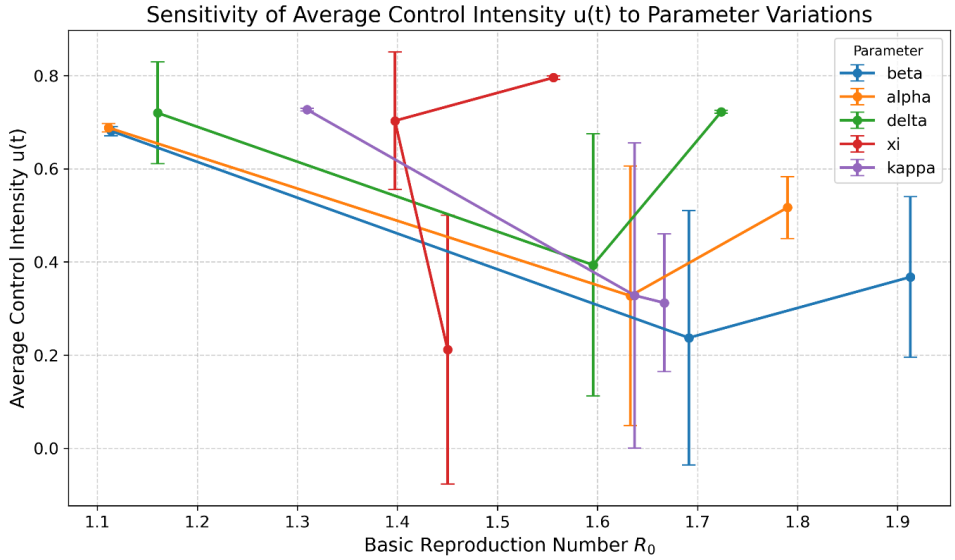

Figure 8: Sensitivity of Average Control Intensity u(t) to Parameter Variations

Figure 9 shows how peak environmental pathogen load B is affected by parameter changes. Both α *and* β have substantial positive relationships with B, highlighting their important roles in fecal-oral transmission. At $R_0 = 1.9$, increasing α or β by 20% increases B by around 50-70%. B is decreased by greater δ and ξ, with δ exhibiting the sharpest fall (~30% reduction at $R_0 = 1.9$). The influence of κ is negligible, indicating that environmental decontamination is less affected by economic limitations.

Received: July 12, 2025

International Journal of Applied Mathematics

Volume 38 No. 1s, 2025

ISSN: 1311-1728 (printed version); ISSN: 1314-8060 (on-line version)

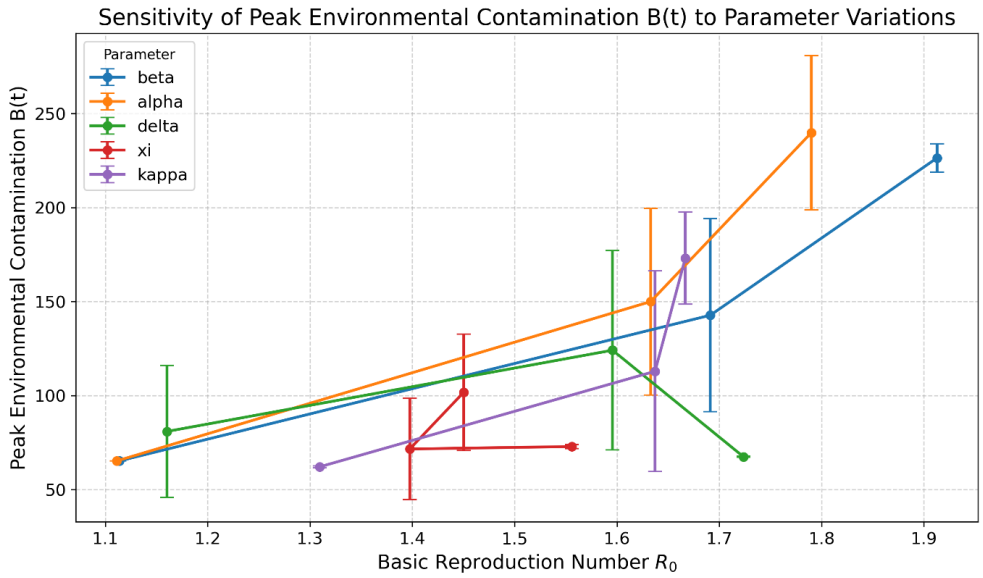

Figure 9: Sensitivity of Peak Environmental Contamination B(t) to Parameter Variations

Figure 10 illustrates parameter-driven variations in the peak infected population, with β and α being important drivers. Peak infections are strongly correlated with β and α, with β accounting for approximately 40% of the variation at $R_0 = 1.9$. Increasing δ or ξ decreases peak infections by around 15-25%, emphasising the relevance of environmental interventions. κ has minimal influence, highlighting the need for behavioural or infrastructure modifications above monetary constraints during outbreak peaks.

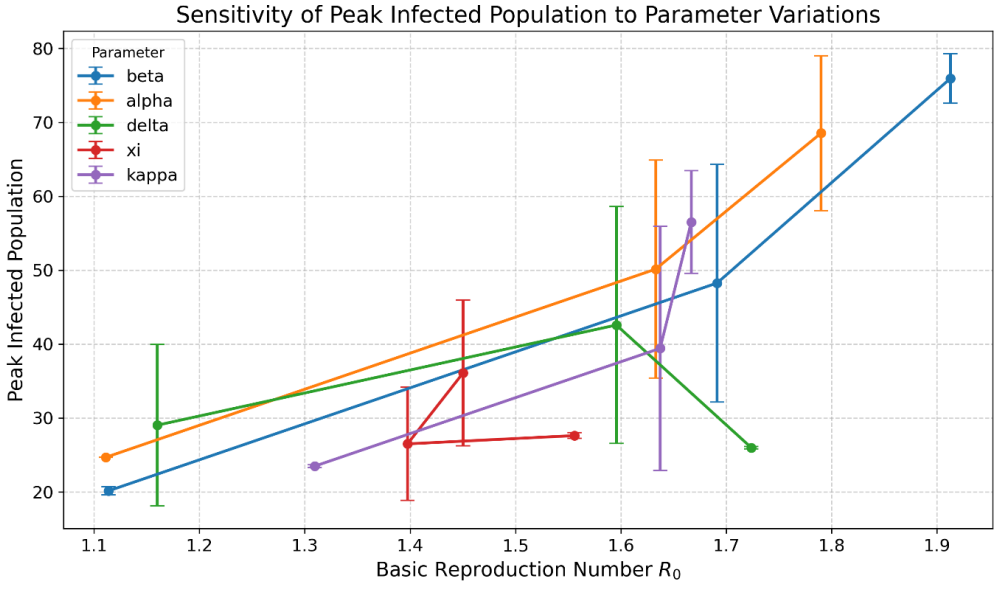

Figure 10: Sensitivity of Peak Infected Population to Parameter Variations

Figure 11 depicts the cumulative infections under various conditions. The importance of β and α in the long-term burden of disease is expressed by their exponential sensitivity; at $R_0 = 1.9$, a 20% increase in β or α increases total infections by around 200–300%. Although δ and ξ

Received: July 12, 2025

International Journal of Applied Mathematics

Volume 38 No. 1s, 2025

ISSN: 1311-1728 (printed version); ISSN: 1314-8060 (on-line version)

lower overall infections, their efficiency decreases with increasing R_0, indicating that environmental measures alone may not be enough to prevent catastrophic outbreaks.

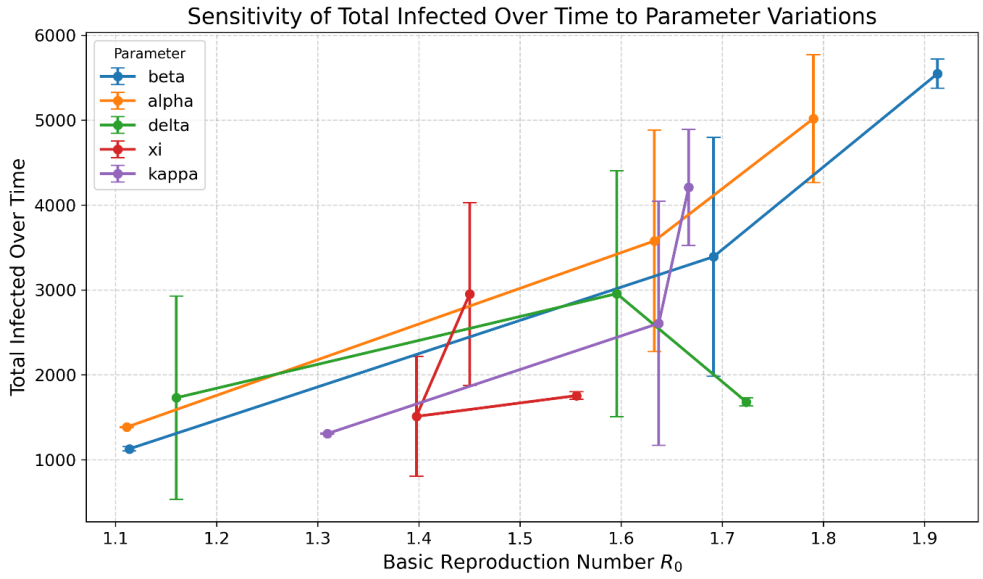

Figure 11: Sensitivity of Total Infected Over Time to Parameter Variations

4. Discussion of results

Open defecation follows a similar trend to the infected population, peaking around the same time. This is because as canvassed in existing studies [40, 41, 42], infected individuals contribute to environmental contamination through open defecation. The simulation results demonstrate the need for long-term, flexible public health measures which will reduce cholera outbreaks and avert secondary infection waves. The model shows that timely sanitation campaigns and behavioural interventions can reduce peak infections by ~60% and environmental pollution by ~40% compared to uncontrolled scenarios by incorporating environmental dynamics such as open defecation and pathogen persistence. This result is consistent with research demonstrating that improvements in WASH (water, sanitation, and hygiene) can lower the incidence of cholera by as much as 73% [13]. A critical window for intervention is highlighted by the optimal control profile ($u(t)$), which emphasises intensive efforts in the first 35 days prior to tapering. By disrupting transmission chains, early suppression of environmental contamination limits susceptible depletion and prevents overload in the healthcare system.

Sensitivity studies also demonstrate how behavioural and biological factors interact. Reductions in contact rates (e.g., handwashing, water treatment) and faecal input (e.g., latrine access) are non-negotiable for prolonged control, as evidenced by the significant positive correlations between transmission rate (β) and defecation contribution (α) and epidemic severity. As mitigating variables, pathogen decay (δ) and removal rate (ξ) have higher values that reduce environmental contamination by 22–30%. This substantiates how technical solutions, including wastewater treatment and chlorination, could quicken pathogen removal.

Received: July 12, 2025

Volume 38 No. 1s, 2025

ISSN: 1311-1728 (printed version); ISSN: 1314-8060 (on-line version)

Also, the model highlights trade-offs between cost and efficiency: whereas high-intensity treatments ($u(t) \geq 0.8$) provide significant short-term advantages, their viability is contingent upon the availability of resources. Policymakers must combine upfront investments (such as infrastructure improvements) with community-led behavioural programs to ensure the long-term adoption of healthier practices. Complementary strategies, such as vaccination to lower vulnerability and media-driven awareness to boost compliance, may further enhance resilience against epidemics.

These results are consistent with field evidence from Asia and sub-Saharan Africa, where cholera endemicity is maintained by insufficient WASH practices [3]. For example, the model's prediction of a 50–70% rise in $B(t)$ under-parameter perturbations reflects actual problems that worsen contamination risks, such as seasonal floods or population displacement. Through a clear connection between open defecation and disease dynamics, the framework emphasises the need for environmental remediation in cholera prevention measures, especially in areas where poverty or cultural norms prevent the adoption of sanitation [13].

5.0 Conclusion

This study proposed a model that combines behavioural factors and environmental pollutants to analyse the dynamics of cholera transmission. Open defecation was explicitly identified as the primary source of pathogen persistence (B) and a temporally adaptive control function ($u(t)$) was incorporated into the model to highlight the critical interplay between human behaviour, environmental reservoirs, and the efficacy of treatments. Thus, a numerical study was conducted to determine the equilibria points, calculate the reproduction number, and investigate their stability. We analysed the criteria for the best management of disease spread and developed the temporally adaptive control ($u(t)$)) utilising Pontryagin's maximum principle. Numerical simulations were performed to demonstrate the analytical results after the optimised system was solved numerically. The numerical simulation results showed that combining infrastructure investment (e.g., wastewater treatment), behavioural nudges (e.g., hygiene education), and environmental remediation (e.g., chlorination) resulted in the optimal level of cholera transmission control and containment. Thus, preventing the spread of cholera necessitates a multipronged strategy. We did not use spatiotemporal heterogeneity (e.g., urban-rural gradients) to improve the forecast for small populations in this study, which leaves room for future research. The study's findings can assist local stakeholders adjust their hygiene efforts to cultural acceptability, minimising cholera's global effect and laying the groundwork for progress towards SDG 6 and health equity in vulnerable regions.

Author contribution statement

Olusegun Olaiju, conceived the idea, Olusegun Olaiju, Olasunkanmi Olapeju and Joshua Kayode Odeyemi, did the writing-original draft, Joshua Kayode Odeyemi, Mukail Akinde, Olasunkanmi Olapeju and Olusegun Olaiju Review & Editing, Olusegun Olaiju formulated the model, Olusegun Olaiju, and Joshua Kayode Odeyemi wrote the coding aspect.

Ethical statement

We wish to confirm that we have adhered to the ethics for publication according to the requirements of Elsevier and COPE.

Received: July 12, 2025

Volume 38 No. 1s, 2025

ISSN: 1311-1728 (printed version); ISSN: 1314-8060 (on-line version)

Funding

The research was not sponsored. Funded. However, The APC was funded by The Federal Polytechnic Ilaro, Ogun State, Nigeria.

Data Availability Statement

The data and formulas that formed the basis of the study's results have been included in the work.

Acknowledgments

We appreciate the Management of the Federal Polytechnic Ilaro, the host institution, for affording us its support through the provision of an enabling environment for the research and funding of the APC.

Conflicts of Interest

The authors declare that they have no known competing financial interests or personal relationships that could have appeared to influence the work reported in this paper.

References

[1] Abubakari, S.W.; Oppong, F.B.; Wiru, K.; Manu, G.; Apraku, E.A.; Abukari, M.; Zandoh, C.; Asante, KP. Open defecation and attainment of Sustainable Development Goal Six: evidence from Kintampo Surveillance System, Ghana. Ghana Med J 2021, 55(4):273-277. doi: 10.4314/gmj.v55i4.

[2] Shehu B, Nazim F. Clean Water and Sanitation for All: Study on SDGs 6.1 and 6.2 Targets with State Policies and Interventions in Nigeria. Environ Sci Proc. 2022;15(1):71. doi:10.3390/environsciproc2022015071.

[3] Okesanya, O.J.; Eshun, G.; Ukoaka, B.M. *et al.* Water, sanitation, and hygiene (WASH) practices in Africa: exploring the effects on public health and sustainable development plans. Trop Med Health 2024, 52, 68. https://doi.org/10.1186/s41182-024-00614-3

[4] Belay, D.G.; Asratie, M.H.; Aragaw, F.M. *et al.* Open defecation practice and its determinants among households in sub-Saharan Africa: pooled prevalence and multilevel analysis of 33 sub-Saharan Africa countries demographic and health survey. Trop Med Health 2022, 50, 28. https://doi.org/10.1186/s41182-022-00416-5.

[5] Giribabu, D.; Bharadwaj, P.; Sitiraju, R.; Burra, M.; Rao, P.; Reddy, C . Combating Open Defecation through Community-led Sanitation. Dr. Sulaiman Al Habib Medical Journal *2019,* 1: (3-4), 45-51.

[6] Olapeju, O.O.; RafeeMajid M. Towards a Sustainable Incentive to Open Defecation Eradication. Journal of Sustainability Science and Management 2019, 15(5), 215-235

[7] Olapeju O. Assessment of the Psychological Dimension to Open Defecation in Ogun State. Environmental Technology & Science Journal 2022, 12(2): 160-170.

[8] Atangana E.; Oberholster P.J. Assessment of water, sanitation, and hygiene target and theoretical modeling to determine sanitation success in sub-Saharan Africa. Environ Dev Sustain 2023, 25(11):13353–77. https://doi.org/10.1007/s10668-022-02620-z.

Received: July 12, 2025

Volume 38 No. 1s, 2025

ISSN: 1311-1728 (printed version); ISSN: 1314-8060 (on-line version)

[9] Tseole, N.P.; Mindu, T. ; Kalinda, C. ; Chimbari, M.J. Barriers and Facilitators to Water, Sanitation and Hygiene (WASH) Practices in Southern Africa: A Scoping Review. PLoS ONE 2022;17(8): e0271726. https://doi.org/10.1371/journal.pone.0271726.

[10] World Health Organisation. Mortality rate attributed to exposure to unsafe WASH services (per 100 000 population) (SDG 3.9.2). 2024. Available online: https://www.who.int/data/gho/data/indicators/indicator-details/GHO/mortality-rate-attributed-to-exposure-to-unsafe-wash-services-(per-100-000-population)-(sdg-3-9-2). Accessed 10-02- 2024.

[11] Mukherjee R, Halder D, Saha S, Shyamali R, Subhranshu C, Ramakrishnan R, Murhekar MV, Hutin YJ. Five pond-centred outbreaks of cholera in villages of West Bengal, India: evidence for focused interventions. J Health Popul Nutr. 2011 Oct;29(5):421-8. doi: 10.3329/jhpn.v29i5.8895. PMID: 22106747; PMCID: PMC3225103.

[12] Ojeda Rodriguez J. A; Hashmi M.F; Kahwaji C.I. Vibrio cholerae Infection. [Updated 2024 May 1]. In: StatPearls [Internet]. Treasure Island (FL): StatPearls Publishing; 2025 Jan-. Available from: https://www.ncbi.nlm.nih.gov/books/NBK526099/

[13] Taylor DL, Kahawita TM, Cairncross S, Ensink JH. The Impact of Water, Sanitation and Hygiene Interventions to Control Cholera: A Systematic Review. PLoS One. 2015 Aug 18;10(8):e0135676. doi: 10.1371/journal.pone.0135676. PMID: 26284367; PMCID: PMC4540465.

[14] Lo Iacono, G.; Nichols, G. Modeling the Impact of Environment on Infectious Diseases. Oxford Research Encyclopedia of Environmental Science 2017. Available online: https://oxfordre.com/environmentalscience/view/10.1093/acrefore/9780199389414.001.0001/acrefore-9780199389414-e-339. (Accessed on 25-03 -2025)

[15] Lanzas C.; Davies, K.; Erwin, S.; Dawson. D. On modelling environmentally transmitted pathogens. Interface Focus 2020, 6;10(1):20190056.

[16] Angelou, A.; Kioutsioukis I.; Stilianakis, N. A climate-dependent spatial epidemiological model for the transmission risk of West Nile virus at local scale. One Health 2021, 13, 2352-7714. https://doi.org/10.1016/j.onehlt.2021.100330.

[17] Anteneh, L.M.; Lokonon, B.E.; Kakaï, R.G. Modelling techniques in cholera epidemiology: A systematic and critical review. Mathematical Biosciences 2024. 373, 0025-5564. https://doi.org/10.1016/j.mbs.2024.109210.

[18] Tien, T.H.; Earn, D.J. Multiple Transmission Pathways and Disease Dynamics In A Waterborne Pathogen Model, B. Math. Biol. 2010, 72, 1506–1533

[19] Mukandavire, Z.; Liao, S.; Wang, J.; Gaff, H.; Smith, D.L; Morris Jr., J.G. Estimating the Reproductive Numbers for the 2008-2009 Cholera Outbreaks in Zimbabwe. Proceedings of the National Academy of Sciences of the United States of America 2011, 108, 8767-8772. https://doi.org/10.1073/pnas.1019712108

[20] Posny, J.; Wang, J. Modeling Cholera in Periodic Environments. J. Biol. Dynam 2014, 8, 1–19.

Received: July 12, 2025

Volume 38 No. 1s, 2025

ISSN: 1311-1728 (printed version); ISSN: 1314-8060 (on-line version)

[21] Wang, X.; Posny , D.; Wang, J. A reaction-convection-diffusion model for cholera spatial dy-namics, Discrete Cont. Dyn. *B* 2016*,* 21, 2785–2809

[22] Wang J. Mathematical Models for Cholera Dynamics-A Review. Microorganisms. 2022 Nov 29;10(12):2358. doi: 10.3390/microorganisms10122358. PMID: 36557611; PMCID: PMC9783556.

[23] Wang, J., & Liao, S. (2012). A generalized cholera model and epidemic–endemic analysis. Journal of Biological Dynamics, *6*(2), 568–589. https://doi.org/10.1080/17513758.2012.658089

[24] Yang, C.; Wang, X.; Gao, D. et al., Impact Of Awareness Programs On Cholera Dynamics: Two Modeling Approaches, B. Math. Biol. 2017, 79, 2109–213

[25] Yang, C.Y.; Wang, J. A. cholera transmission model incorporating the impact of medical resources. Math Biosci Eng. 2019, 6;16(5):5226-5246. doi: 10.3934/mbe.2019261. PMID: 31499710.

[26] Durojaye, M.O.; Odeyemi, J.K.. Radial Basis Function - Finite Difference (RBF-FD) Approximations for Two-Dimensional Heat Equations. Pacific Journal of Science and Technology 2019, 20(2), 43–49.

[27] Olaiju, O.A.; Hoe, Y.S.; Ogunbode, E.B. Finite Element and Finite Difference Numerical Simulation Comparison for Air Pollution Emission Control to Attain Cleaner Environment". Chemical Engineering Transactions 2018, 63, 625–630. DOI: 10.3303/CET1863105.

[28] Kamgang, J.C.; Sallet, G. Computation of threshold conditions for epidemiological models and global stability of the disease-free equilibrium (DFE). Mathematical Biosciences 2008, 213 (1), 1-12.

[29] Tewa, J.J.; Fokouop, R.; Mewoli, B.; Bowong, S. Mathematical Analysis of a General Class of Ordinary Differential Equations Coming From Within-hosts Models of Malaria With Immune Effectors, Applied Mathematics and Computation 2012, 218, 14, 7347-7361.

[30] Akbari, R.; Kamyad, Av.; Heydari, A.A.; Heydari, A. The Analysis of a Disease-Free Equilibrium of Hepatitisb Model SCMA 2016, 3 (2),1-11.

[31] Almeida, R.; Martins, N.; Silva, C. J. Global Stability Condition for the Disease-Free Equilibrium Point of Fractional Epidemiological Models. Axioms *2021,*10*(4), 238. https://doi.org/10.3390/axioms10040238*

[32] Liao, S.; Wang, J. Stability analysis and Application of a Mathematical Cholera Model. Mathematical Biosciences And Engineering 2011, 8 (3), 733752

[33] van den Driessche P, Watmough J. Reproduction numbers and sub-threshold endemic equilibria for compartmental models of disease transmission. Math Biosci. 2002 Nov-Dec;180:29-48. doi: 10.1016/s0025-5564(02)00108-6. PMID: 12387915.

[34] Suryani, L.;Kusumawinahyu, W.M.; Shofianah, N. Dynamical Analysis on A Model of Cholera Epidemic with Quarantine, Vaccination, and Two Path of Transmissions. J. Phys 2021, Conf. Ser. *1776 012052*

Received: July 12, 2025

Volume 38 No. 1s, 2025

ISSN: 1311-1728 (printed version); ISSN: 1314-8060 (on-line version)

[35] Brhane, K.W.; Ahmad, A.G.; Hina, H. *et al.* Mathematical modeling of cholera dynamics with intrinsic growth considering constant interventions. Sci Rep 2024 14, 4616 https://doi.org/10.1038/s41598-024-55240-0

[36] Yaseen, R.M.; Ali, N.F.; Mohsen, A.A.; Khan, A.; Abdeljawad, T. The Modeling and Mathematical Analysis of the Fractional-Order of Cholera disease: Dynamical and Simulation, Partial Differential Equations in Applied Mathematics 2024, 12, 100978.

[37] Agusto FB, Del Valle SY, Blayneh KW, Ngonghala CN, Goncalves MJ, Li N, Zhao R, Gong H. The impact of bed-net use on malaria prevalence. J Theor Biol. 2013 Mar 7;320:58-65. https://doi.org/10.1016/j.jtbi.2012.12.007. Epub 2012 Dec 13. PMID: 23246718; PMCID: PMC3623563

[38] McLean AR. Infectious Disease Modeling. Infectious Diseases. 2012 Dec 5:99–115. https://doi.org/10.1007/978-1-4614-5719-0_5 . PMCID: PMC7121366.

[39] Niu Y, et al. Containing the transmission of COVID-19: A modeling study in 160 countries. Front Med. 2021;8:701836. https://doi.org/10.3389/fmed.2021.701836

[40] Brouwer, A.F., Eisenberg, M.C., Love, N.G. *et al.* Phenotypic variations in persistence and infectivity between and within environmentally transmitted pathogen populations impact population-level epidemic dynamics. BMC Infect Dis **19**, 449 (2019). https://doi.org/10.1186/s12879-019-4054-8

[41] Okullo, J.O.; Moturi, W.N.; Ogendi, G.M. Open Defaecation and Its Effects on the Bacteriological Quality of Drinking Water Sources in Isiolo County, Kenya. Environ Health Insights 2017, 9;11:1178630217735539. doi: 10.1177/1178630217735539

[42] Saleem, M.; Burdett, T.; Heaslip, V. Health and social impacts of open defecation on women: a systematic review. BMC Public Health 2019, 19, 158 https://doi.org/10.1186/s12889-019-6423-z

[43] Sun, S.; Han, J. Open Defecation and Squat Toilets, An Overlooked Risk of Fecal Transmission of COVID-19 and other pathogens in developing communities. *Environ Chem Lett* 2021, 19, 787–795. https://doi.org/10.1007/s10311-020-01143-1

[44] Odeyemi JK, Olaiya OO, Ogunfiditimi FO. Hermite Polynomial-based Methods for Optimal Order Approximation of First-order Ordinary Differential Equations. *J* Adv Math Comput Sci. 2023;38(6):16-32. doi:10.9734/jamcs/2023/v38i6814

Received: July 12, 2025